Isolation and Characterization of New Anti-Inflammatory and Antioxidant Components from Deep Marine-Derived Fungus *Myrothecium* sp. Bzo-l062

Xiaojie Lu [1,2,†], Junjie He [1,†], Yanhua Wu [3], Na Du [1], Xiaofan Li [1], Jianhua Ju [4], Zhangli Hu [1,2], Kazuo Umezawa [3,*] and Liyan Wang [1,*]

1   Shenzhen Key Laboratory of Marine Bioresource and Eco-environmental Science,
    College of Life Sciences and Oceanography, Shenzhen University, Shenzhen 518060, China;
    luxiaojie@szu.edu.cn (X.L.); hejunjie2017@email.szu.edu.cn (J.H.); duna2017@email.szu.edu.cn (N.D.);
    lixiaof@szu.edu.cn (X.L.); huzl@szu.edu.cn (Z.H.)
2   Key Laboratory of Optoelectronic Devices and Systems of Ministry of Education and Guangdong Province,
    College of Optoelectronic Engineering, Shenzhen University, Shenzhen 518060, China
3   Department of Molecular Target Medicine, Aichi Medical University School of Medicine,
    Nagakute 480-1195, Japan; wu.yanhua.196@mail.aichi-med-u.ac.jp
4   CAS Key Laboratory of Tropical Marine Bio-resources and Ecology, South China Sea Institute of Oceanology,
    Chinese Academy of Sciences, Guangzhou 510301, China; jju@scsio.ac.cn
*   Correspondence: umezawa@aichi-med-u.ac.jp (K.U.); lwang@szu.edu.cn (L.W.);
    Tel.: +81-561-61-1959 (K.U.); +86-755-2601-2653 (L.W.)
†   These authors contributed equally to this work.

check for updates

Abstract: In the present study, four new compounds including a pair of 2-benzoyl tetrahydrofuran enantiomers, namely, (−)-1*S*-myrothecol (**1a**) and (+)-1*R*-myrothecol (**1b**), a methoxy-myrothecol racemate (**2**), and an azaphilone derivative, myrothin (**3**), were isolated along with four known compounds (**4–7**) from cultures of the deep-sea fungus *Myrothecium* sp. BZO-L062. Enantiomeric compounds **1a** and **1b** were separated through normal-phase chiral high-performance liquid chromatography. The absolute configurations of **1a**, **1b**, and **3** were assigned by ECD spectra. Among them, the new compound **1a** and its enantiomer **1b** exhibited anti-inflammatory activity, inhibited nitric oxide formation in lipopolysaccharide-treated RAW264.7 cells, and exhibited antioxidant activity in the 2,2-azino-bis(3-ethylbenzothiazoline-6-sulfonic acid) and oxygen radical absorbance capacity assays.

Keywords: deep sea marine-derived fungus; *Myrothecium* sp.; myrothecol; nitric oxide (NO); antioxidant activity

---

1. Introduction

Natural products are a rich source of new drugs and they are frequently used for the discovery and development of new drugs [1]. Natural marine products with unique architectures and distinct biological activities are treasure troves for natural product chemists [2,3]. Among marine organisms, fungi produce a diverse range of biologically active metabolites [3], including polyketides [4–6], terpenoids [7–9], polypeptides [10], and alkaloids [11–13].

Microorganisms of the deep-sea are an attractive source of candidate drugs. While screening inhibitors of lipopolysaccharide (LPS)-induced nitric oxide (NO) production, we recently isolated cyclopenol and cyclopenin from the extract of the fungal strain *Aspergillus* sp. SCSIOW2 collected from a depth of approximately 2000 m in the sea [14]. At non-toxic concentrations, these compounds

inhibited LPS-induced NO production and IL-6 secretion in RAW264.7 cells. This inhibitory effect of cyclopenol and cyclopenin was attributed to the suppression of the upstream signal of NF-B activation. These compounds also suppressed the expression of IL-1β, IL-6, and iNOS in microglia cells (macrophages in the mouse brain) [14]. In Alzheimer's disease, amyloid β-peptide induces inflammation in the brain. Between the two compounds, cyclopenin showed ameliorative effects in an in vivo Alzheimer's model using flies [14].

To explore new bioactive secondary metabolites from deep marine-derived fungi [15–17], a fungal strain, *Myrothecium* sp. BZO-L062, isolated from sediment samples collected from the sea bottom near Yongxing Island, was used for chemical investigation. Seven pure components, including four new compounds (**1a**, **1b**, **2**, and **3**), were isolated and identified from the ethyl acetate extract of the fungus (Figure 1). The absolute configurations of the new compounds (**1a**, **1b**, and **3**) were assigned by comparison of their experimental CD spectra with the theoretically calculated spectra. The NO production inhibitory activity and antioxidant activity of the new compounds were also evaluated. Known compounds **4**–**7** were identified as terreinol (**4**) [18], 3,5-dihydroxy-4-methylbenzoic acid methyl ester (**5**), 5-hydroxymethyl-2-furoic acid (**6**) [19], and 5-hydroxymethyl-2-furancarboxylic acid methyl ester (**7**) [20] by comparing their spectroscopic data with those previously reported.
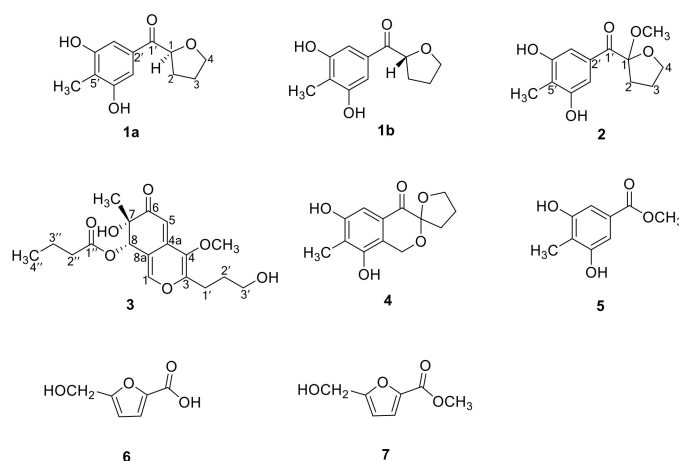
Figure 1. Compounds **1**–**7** isolated from *Myrothecium* sp. BZO-L062, including (−)-(1*S*)-myrotheciol (**1a**), (+)-(1*R*)-myrotheciol (**1b**), 1-methoxy-myrotheciol (**2**), myrothin (**3**), terreinol (**4**), 3,5-dihydroxy-4-methylbenzoic acid methyl ester (**5**), 5-hydroxymethyl-2-furoic acid (**6**), and 5-hydroxymethyl-2-furancarboxylic acid methyl ester (**7**).

2. Results and Discussion

The molecular formula of **1** was determined as $C_{12}H_{14}O_4$ by high-resolution electrospray ionization mass spectrometry (HRESIMS) at *m/z* 223.0958 [M + H]$^+$ and 245.0780 [M + Na]$^+$ (calculated for $C_{12}H_{15}O_4{}^+$, 223.0965; $C_{12}H_{14}O_4Na^+$, 245.0784) (Figure S1). ^{1}H NMR, ^{13}C NMR, and 2D-NMR data of **1** (Table 1, Figures S2–S8) revealed the presence of 12 resonance signals, including those for one sp^3 methyl, one sp^3 oxygenated methine, three sp^3 methylenes, two symmetric sp^2 methines, two symmetric sp^2 oxygenated quaternary carbons, two sp^2 quaternary carbons, and one ketone carbonyl carbon. The ^{1}H-^{1}H correlation spectroscopy (COSY) data from H-1 to H$_2$-4 and the ^{1}H-^{13}C heteronuclear multiple bond correlations (HMBC) from H-1 to oxygenated C-4 and from H$_2$-4 to C-1 suggested the presence of a tetrahydro-2-furanyl moiety (Table 1 and Figure 2). The four aromatic carbon signals indicated the presence of one symmetrically substituted benzene ring. The HMBC experiment correlations confirmed the presence of a 3,5-dihydroxy-4-methyl benzoyl moiety (Table 1 and Figure 2). Finally, the key HMBC correlations from H$_2$-2 to C-1 and from H-1 to C-2 allowed the linkage of the 3,5-dihydroxy-4-methyl benzoyl and tetrahydro-2-furanyl groups (Table 1 and Figure 2).

Accordingly, **1** was established as (3,5-dihydroxy-4-methylphenyl)-(tetrahydro-2-furanyl)methanone and denoted as a myrotheciol.

Table 1. ^{1}H NMR (600 MHz) and ^{13}C NMR (150 MHz) spectral data of **1**.

No.	δ_C	δ_H, Mult. (*J* in Hz)	^{1}H-^{1}H COSY	HMBC
1	79.1	5.09, dd (8.4, 5.6)	2	C-2,3,4
2	29.0	2.17, m; 1.92, m	1,3	C-1,3,4,1′
3	25.2	1.84, m	2,4	C-1,2,4
4	68.4	3.81, t (6.7)	3	C-1,2,3
1′	198.0	-		
2′	132.7	-		
3′,7′	106.1	6.92, s		C-1′,2′,4′(6′),5′
4′,6′	156.1	-		
5′	116.7	-		
4′−OH/6′−OH	-	9.51, s		C-3′,4′,5′/C-5′,6′,7′
5′−CH$_3$	8.9	1.99, s		C-4′,5′,6′
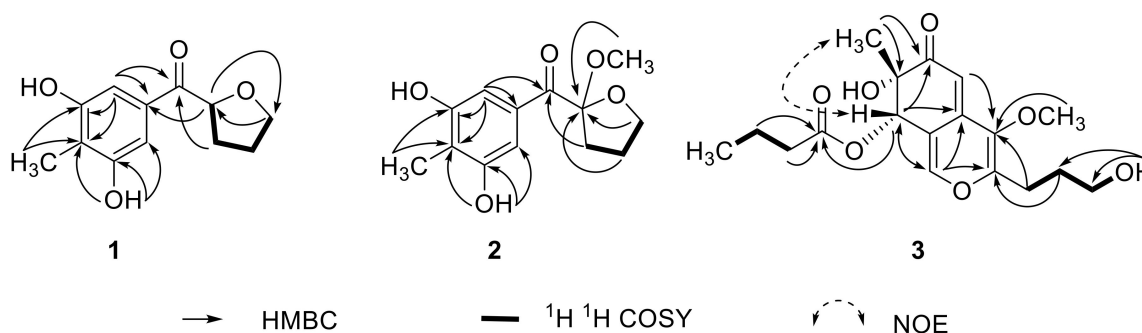
Figure 2. Key 2D NMR correlations of **1**–**3**.

The absence of the Cotton effect in the CD spectrum and zero specific rotation indicated that **1** was a racemate. Generally, enantiomers are more advantageous than racemates for drug development. To detect the enantiomers of **1**, chiral HPLC was performed using a Chiralpak IC column; the HPLC results showed two separate peaks (Figure S9). The two enantiomers, (−)-**1a** and (+)-**1b**, were obtained in a ratio of 1:1. (−)-**1a** and (+)-**1b** showed mirror image-like CD curves (Figure 3) and opposite specific rotations (**1a**: $[\alpha]_D^{20}$ − 25.3; **1b**: $[\alpha]_D^{20}$ + 26.3). The experimental CD spectra of **1a** were consistent with the theoretically calculated ECD spectrum of the **1**-*S* enantiomer with four Cotton effects observed at 237 nm (positive), 270 nm (positive), 310 nm (negative), and 348 nm (positive) (Figure 3). In contrast, the CD spectrum of **1b** was consistent with the ECD spectrum of the 1-*R* enantiomer but different from that of **1**-*S* with three negative Cotton effects at 237 nm, 270 nm, and 348 nm, and one positive Cotton effect at 310 nm. Thus, the absolute configurations of **1a** and **1b** were assigned as (−)-(1*S*)-myrotheciol and (+)-(1*R*)-myrotheciol, respectively (Figure 1).

The molecular formula of **2** was determined as $C_{13}H_{16}O_5$ through HRESIMS at *m/z* 275.0896 [M + Na]$^+$ (calculated for $C_{13}H_{16}O_5Na^+$, 275.0890), which was 30 mass units larger than **1** (Figure S10). The ^{1}H and ^{13}C NMR data of **2** (Table 2, Figures S11–S16) closely resembled those of **1**, except for three major differences: the presence of an additional methoxy group (δ_H 3.09, δ_C 50.2), the absence of a methine proton (δ_H 5.09), and the chemical shift of C-1 (from δ_C 79.1 to 109.5); these differences indicated the substitution of the methine proton at C-1 by a methoxy group. The position of the new methoxy group was confirmed by HMBC correlation from 1-OMe to C-1 (Table 2 and Figure 2). Thus, **2** was established as 1-methoxy-myrotheciol. The structure of **2** was validated through a detailed analysis of 2D NMR data (Table 2 and Figure 2).
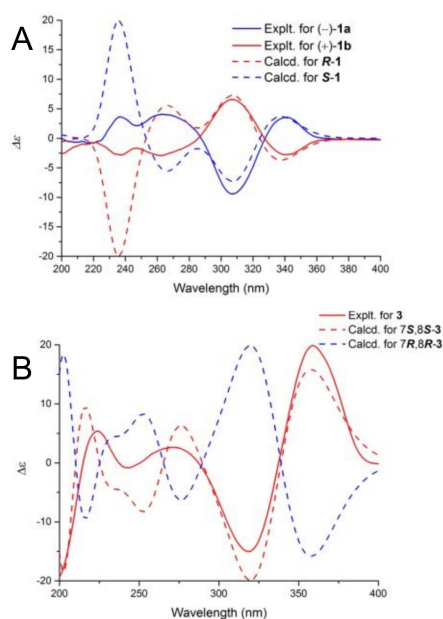
Figure 3. ECD spectra of compounds **1a** and 1b (**A**), and **3**(**B**).

Table 2. ^{1}H NMR (600 MHz) and ^{13}C NMR (150 MHz) spectral data of **2**.

No.	δ_C	δ_H, Mult. (*J* in Hz)	^{1}H-^{1}H COSY	HMBC
1	109.5	-		
2	34.6	2.13, m	3	C-1,3,4,1′
3	24.0	1.88, m; 2.01, m	2,4	C-1,2,4
4	68.1	3.96, m	3	C-1,2,3
1′	194.8	-		
2′	131.7	-		
3′,7′	107.3	7.09, s		C-1′,2′,4′(6′),5′
4′,6′	155.9	-		
5′	116.7	-		
1−OCH$_3$	50.2	3.09, s		C-1
4′−OH/6′−OH	-	9.47, s		C-3′,4′,5′/ C-5′,6′,7′
5′−CH$_3$	8.9	1.98, s		C-4′,5′,6′

Compound **2** was also considered as a racemic mixture based on the zero specific rotation and absence of the Cotton effect in its CD spectrum. The chiral HPLC performed using the same condition as that used for **1** revealed two peaks, attributable to **2a** and **2b**, at a ratio of approximately 1:1 (Figure S17). However, due to the limited sample size, further isolation was not carried out.

(+)-HRESIMS at *m/z* 353.1599 [M + H]$^+$ and 375.1418 [M + Na]$^+$ (calculated for $C_{18}H_{25}O_7{}^+$, 353.1595; $C_{18}H_{24}O_7Na^+$, 375.1414) revealed the molecular formula of **3** as $C_{18}H_{24}O_7$ (Figure S18). The 1D- and 2DNMR results revealed the presence of one sp^3 oxygenated quaternary carbon, one sp^3 oxygenated methine, two sp^2 aromatic methines, four sp^2 quaternary carbons, one ketone carbonyl carbon, one methoxy group, and one angular methyl group (Table 3 and Figures S19–25). Other than these signals, the ^{1}H-^{1}H COSY correlations from H-2″ to H-4″, along with the HMBC correlations from H-2″ and 3″ to C-1″ (Table 3 and Figure 2) indicated the presence of the butyl ester fragment. The ^{1}H-^{1}H COSY correlations from H-1 to 3-OH corresponded to the hydroxypropyl fragment (Table 3, Figure 2). The NMR data of the core structure of **3** closely resembled those of C-8 dihydro-azaphilone [21,22]. Careful HMBC analysis confirmed this structure (Table 3 and Figure 2). Finally, the key HMBC correlation from H-8 to C-1″connected the butyl ester side chain to C-8, that from H-1 and H-2 to

C-3 connected the hydroxypropyl group moiety to C-3, and that from 4-OCH$_3$ to C-4 connected the methoxy group to C-4 (Table 3 and Figure 2). Accordingly, **3** was established as myrothin (Figure 1).

Table 3. ^{1}H NMR (600 MHz) and ^{13}C NMR (150 MHz) data of **3**.

No.	δ_C	δ_H, Mult. (*J* in Hz)	^{1}H-^{1}H COSY	HMBC
1	146.9	7.66, d (1.2)		C-3,4a,8,8a
3	154.7	-		
4	138.3	-		
4a	139.6	-		
5	99.7	5.28, d (1.2)		C-4,7,8a
6	196.5	-		
7	73.29	-		
8	73.30	5.54, s		C-1,4a,6,7,8a,1″
8a	116.5	-		
1′	24.2	2.58, m	2′	C-3,4,2′,3′
2′	29.6	1.68, m	1′,3′	C-3,1′,3′
3′	59.88	3.44, m	2′,3′-OH	C-1′,2′
3′-OH	-	4.58, t (5.1)	3′	C-2′,3′
4-OCH$_3$	59.94	3.62, s		C-4
7-CH$_3$	23.4	1.16, s		C-6,7
7-OH	-	5.07, s		C-6,7,7-CH$_3$
1″	172.2	-		
2″	35.4	2.26, t (7.2)	3″	C-1″,3″,4″
3″	17.9	1.49, m	2″, 4″	C-1″,2″,4″
4″	13.2	0.82, t (7.4)	3″	C-2″,3″

The relative configuration of **3** at C-7 and C-8 was assigned by nuclear overhauser effect spectroscopy (NOESY) correlations. The strong NOESY correlation between 7-CH$_3$ and H-8 indicated that 7-CH$_3$ and H-8 occupied the same side of the ring (Figure 2 and Figure S25). Thus, the stereo-configurations of C-7 and C-8 are either *S,S* or *R,R*. The experimental ECD curve of **3** was consistent with that of the 7*S*, 8*S* epimer (Figure 3). The chiral carbons C-7 and C-8 were thus determined as 7*S* and 8*S*.

LPS-induced NO production in RAW264.7 cells was used to evaluate the anti-inflammatory activity of different compounds [14]. NO is produced by NF-κB-dependent inducible NO synthase. All the isolated compounds were evaluated for cytotoxicity and for their effects on LPS-induced NO production. Among all the tested compounds, only two new compounds (**1a** and **1b**) significantly inhibited LPS-induced NO production at non-toxic concentrations (Figure 4).

Antioxidant activities were measured through 2,2-azino-bis(3-ethylbenzothiazoline-6-sulfonic acid) (ABTS) scavenging activity, 1,1-diphenyl-2-picrylhydrazyl (DPPH) scavenging capacity, and the oxygen radical absorbance capacity (ORAC) assay. As shown in Table 4, new compounds **1a** and **1b** exhibited antioxidant activity in the ABTS assay with EC$_{50}$ of 1.20 and 1.41 µgmL^{-1}, respectively, which were comparable with EC$_{50}$ values of the positive controls L-ascorbic acid (1.55 µgmL^{-1}) and trolox (1.61 µgmL^{-1}). In the ORAC assay, the antioxidant ability was expressed as µmol trolox equivalents per µmol of sample solution. Compounds **1a** and **1b** showed high antioxidant activity (1.41 µM trolox/µM for **1a** and 1.19 µM trolox/µM for **1b**). Generally, the scavenging activities of ABTS are significantly higher than the scavenging activities of DPPH in phenolic compounds [23]. Compounds **1a** and **1b** did not show antioxidant activity in the DPPH assay, even at the highest concentration of 10 µgmL^{-1}.

In the present research, we isolated several compounds including new structures from a deep-sea fungus. We found cellular anti-inflammatory activity in **1a** and **1b**. Microorganisms often produce useful compounds for therapy. However, the role of these compounds on producing organisms is not clear. At the beginning of antibiotic research, antibiotics are considered to protect the producing organisms by killing their enemy microorganisms. But later, many enzyme inhibitors such as pepstatin and leupeptin were discovered from the secondary metabolites of *Streptomyces*, and they showed

no antibiotic activity. Therefore, it is unlikely that these secondary metabolites are useful for the producers. From this point of view, new compounds, **1a** and **1b**, may be remnants of microorganisms in their evolution.
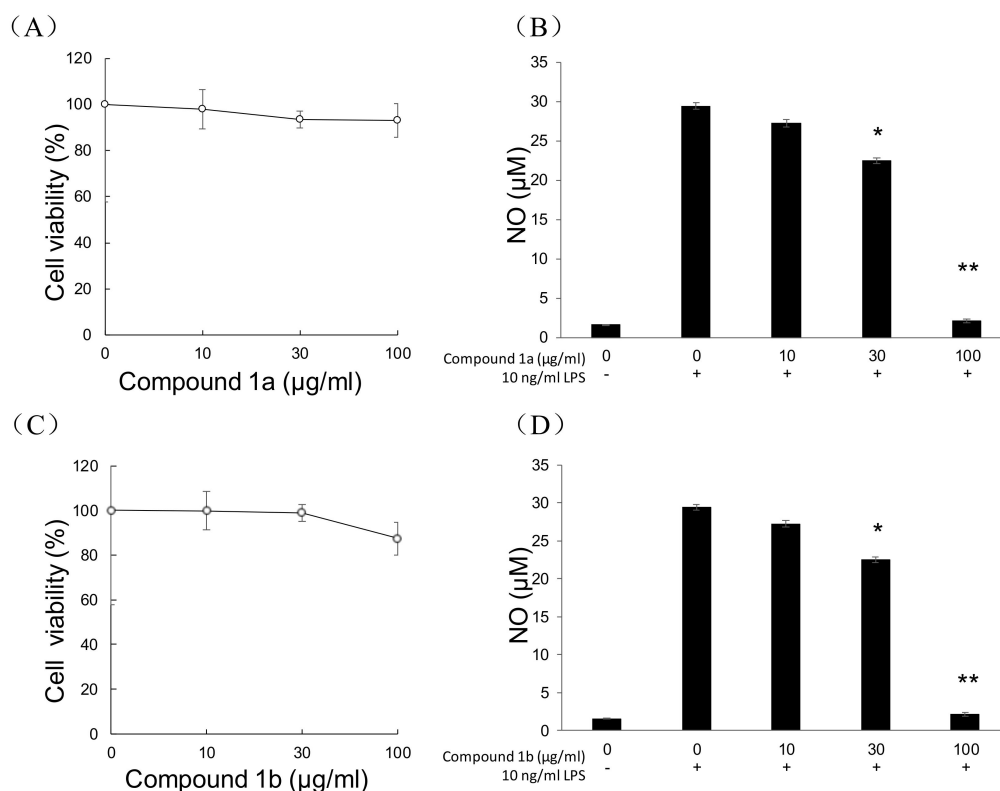
Figure 4. NO production inhibitory activity of **1a** and **1b** in RAW264.7 cells. Effect of **1a** (**A**) or **1b** (**C**) on the viability of RAW264.7 cells. Inhibition of LPS-induced NO production by **1a** (**B**) or **1b** (**D**). Values represent the means ± SEM of three independent experiments. *, $p < 0.05$; **, $p < 0.001$ vs. control.

Table 4. Antioxidant activities of **1a** and **1b**.

Compounds	ABTS	ORAC
	EC$_{50}$, µg/mL	µM Trolox Equivalent/µM
1a	1.20 ± 0.18	1.41 ± 0.27
1b	1.41 ± 0.19	1.19 ± 0.19
L-Ascorbic acid	1.55 ± 0.15	0.35 ± 0.14
Trolox	1.61 ± 0.09	NA

3. Materials and Methods

3.1. General Experimental Procedures

Optical rotations were recorded on an Anton Paar MCP-100 polarimeter (Anton Paar GmbH, Graz, Austria). ECD spectra were measured on a JASCO-810 spectropolarimeter (JASCO Corporation, Tokyo, Japan). UV spectra were obtained on a UV-1800 spectrophotometer (Shimadzu Corporation, Tokyo, Japan). IR spectra were recorded on a Nicolet Avatar 330 FT-IR spectrometer (Thermo Scientific, Waltham, MA, USA) using KBr disks. NMR spectra were acquired on a Bruker ASCEND 500 MHz or 600 MHz NMR magnet system (Bruker, Ettlingen, Germany) using tetramethylsilane (TMS) as the internal standard. HRESIMS was performed using a Triple TOF 6600 (AB SCIEX LLC, Framingham, MA, USA). Column chromatography (CC) was conducted using silica gel (200–300 mesh,

Qingdao Marine Chemical Factory, Qingdao, China) and Sephadex LH-20 (Amersham Pharmacia Biotech, Piscataway, NJ, USA). Thin-layer chromatography (TLC) was performed on Merck TLC plates silica gel 60 F_{254} and silica gel 60 RP-18 F_{254S} (Merck Millipore Corporation, Darmstadt, Germany). HPLC was carried out on a Shimadzu LC-16P HPLC system (Shimadzu Corporation, Tokyo, Japan) using YMC-pack Pro C18 Column (4.6 × 250 mm, 5 μm; 10 × 250 mm, 5 μm; YMC Co., Ltd., Kyoto, Japan) for analysis and semi-preparation. Optical pure compounds were prepared using a DAICEL Chiralpak IC column (250 mm × 4.6 mm, 5 μm; YMC Co., Ltd., Kyoto, Japan). All the chemical reagents for isolation were either of analytical (Damao Chemical Factory, Tianjin, China) or HPLC grade (Kermel Chemical Co., Ltd., Tianjin, China).

3.2. Fungal Material

The fungus *Myrothecium* sp. BZO-L062 used in this study was isolated from a deep-sea (2130 m depth) sediment sample collected from an area close to Yongxing Island, China. The strain was identified as *Myrothecium* sp. based on the morphological features and internal transcribed spacer sequence analysis. This strain was deposited at the Marine Natural Products Laboratory, College of Life Sciences and Oceanography, Shenzhen University, Shenzhen, China.

3.3. Fermentation and Extraction

The fungus *Myrothecium* sp. BZO-L062 was activated on petri dishes containing potato dextrose agar supplemented with 3% sea salt at 28 °C for three days [24]. Agar plugs were inoculated in a 500 mL Erlenmeyer flask containing 150 mL of liquid potato dextrose culture medium [24] supplemented with 3% sea salt as seed cultures and were incubated at 28 °C on a rotary shaker at 180 rpm for three days. Large-scale fermentation (70 L) was conducted using the same medium as that for seed cultures at 28 °C and 180 rpm for seven days. After seven days, the fermentation broth was filtered through cheesecloth to separate the supernatant from the mycelia. The supernatant was then concentrated to 8 L and successively extracted three times with EtOAc (3 × 8 L), yielding a crude extract (40.0 g).

3.4. Isolation and Purification

The crude extract was separated using silica gel CC through CH_2Cl_2/MeOH gradient elution (100:0, 100:1, 100:5, 100:10, 100:20, 100:50, and 0:100; 600 mL each) and was grouped into nine fractions (Fr.) based on the TLC analysis (Fr.1 to Fr.9). Fr.3 was purified by semi-preparative HPLC (28% MeCN/H_2O, flow rate 3 mLmin^{-1}) to yield **4** (t_R 16.2 min, 10.1 mg). Fr.4 was subjected to HPLC using a medium-pressure octadecyl-silica (ODS) column and separated with MeOH/H_2O (20–100%) into five fractions (Fr.4.1–Fr.4.5). Fr.4.1 was further fractionated by HPLC (5% MeOH/H_2O, a flow rate of 3 mLmin^{-1}) to obtain **6** (t_R 15.0 min, 5.0 mg) and **7** (t_R 24.0 min, 5.0 mg). Fr.4.2 was purified by HPLC (25% MeOH/H_2O, a flow rate of 3 mLmin^{-1}) to obtain **3** (t_R 21.0 min, 1.0 mg). Fr.4.3 was refined by HPLC (25% MeCN/H_2O, a flow rate of 3 mLmin^{-1}) to obtain **2** (t_R 20.0 min, 1.4 mg). Finally, Fr.5 was subjected to HPLC (17% MeCN/H_2O, flow rate 3 mLmin^{-1}) to obtain **1** (t_R 20.0 min, 14.2 mg) and **5** (t_R 21.2 min, 10.2 mg).

The racemic compound **1** was resolved into enantiomers (−)-**1a** (3.0 mg, t_R 10.2 min) and (+)-**1b** (3.6 mg, t_R 18.1 min) using a chiral HPLC equipped with a DAICEL® Cellulose Chiralpak IC column (5 μm, 4.6 × 250 mm) using *n*-hexane-ethanol (89:11) as mobile phase at a flow rate of 1 mLmin^{-1}.

3.5. Spectral Data of the Compounds

3.5.1. (±)-Myrothecol (1)

Myrothecol (**1**) is a colorless oil; $[\alpha]_D^{20}$ 0°(*c* 0.1, MeOH); UV (MeOH) λ$_{max}$ (log ε) 280 nm (7.18) and 218 nm (7.46); IR (KBr) ν$_{max}$ 3325, 2956, 1678, 1591, 1423, 1325, 1198, 1088, 1040, 934, and 851; HRESIMS *m/z* 223.0958 [M+H]$^+$, 245.0780 [M+Na]$^+$ (calculated for $C_{12}H_{15}O_4$, 223.0965; $C_{12}H_{14}O_4Na$, 245.0784); for ^{1}H NMR (DMSO-*d$_6$*, 600 MHz) and ^{13}C NMR (DMSO-*d$_6$*, 150 MHz) spectral data, see Table 1.

(−)-**1a**: $[\alpha]_D^{20}$—25.3° (*c* 0.3, MeOH); ECD (2.3 mM, MeOH) λ_{max} (Δε) 237 nm (+0.49), 262 nm (+0.54), 307 nm (−1.27), 341 nm (+0.48). (+)-**1b**: $[\alpha]_D^{20}$ + 26.3° (*c* 0.27, MeOH); ECD (2.3 mM, MeOH) λ_{max} (Δε) 237 nm (−0.38), 262 nm (−0.39), 307 nm (+0.88), and 341 nm (−0.37).

3.5.2. Methoxy-myrothecol (2)

Methoxy-myrothecol (**2**) is a colorless oil; $[\alpha]_D^{20}$ 0° (*c* 0.1, MeCN); UV (MeOH) λ_{max}(log ε) 285 nm (6.99) and 218 nm (7.24); HRESIMS *m/z* 275.0896 [M+Na]$^+$ (calculated for $C_{13}H_{16}O_5Na$, 275.0890); HRESIMS *m/z* 353.1599 [M+H]$^+$, 375.1418 [M+Na]$^+$ (calculated for $C_{18}H_{25}O_7$, 353.1595; $C_{18}H_{24}O_7Na$, 375.1414); for ¬^{1}H NMR (DMSO-*d*$_6$, 600 MHz) and ^{13}C NMR (DMSO-*d*$_6$, 150 MHz) spectral data, see Table 2.

3.5.3. Myrothin (3)

Myrothin (**3**) is a light-yellow colored oil; UV (MeOH) λ_{max} (log ε) 246 nm (3.13) and 350 nm (3.56); IR (KBr) ν_{max} 3405, 2925, 2376, 2316, 1621, 1385, 1036, 910, 790, 731, and 635 cm^{-1}; HRESIMS m/z 353.1599 [M+H]$^+$, 375.1418 [M+Na]$^+$, 727.2948 [2M+Na]$^+$ (calculated for $C_{18}H_{25}O_7$, 353.1595; $C_{18}H_{24}O_7Na$, 375.1414; $C_{36}H_{48}O_{14}Na$, 727.2936); for ¬^{1}H NMR (DMSO-*d*$_6$, 600 MHz) and ^{13}C NMR (DMSO-*d*$_6$, 150 MHz) spectral data, see Table 3. $[\alpha]_D^{20}$ + 15.7°; ECD (2.8 mM, MeOH) λ_{max} (Δε) 224 nm (+0.7), 243 nm (−0.11), 271 nm (+0.34), 319 nm (+1.96), and 359 nm (+2.59).

3.6. ECD Calculation

The conformational distribution search was conducted with the MMFF94 molecular mechanics force field in Spartan 12 software (Wavefunction Inc., Irvine, CA, USA). The lowest energy conformers within the 5-kcalmol^{-1} energy window were optimized using the Gaussian 09 program [25]. TDDFT calculations for all optimized conformers were performed at the B3LYP/6-31G (d, p) level. The ECD spectra were generated using the software SpecDis [26].

3.7. MTT and NO Production Assay

MTT and NO production inhibitory activities of the isolated compounds in RAW264.7 cells were determined as reported previously [14].

3.8. Antioxidant Activity

The ABTS and DPPH scavenging assays were carried out as reported earlier [23]. L-ascorbic acid and trolox were used as positive controls. The ORAC assay was conducted according to a previously reported protocol [27]. The results were expressed as μmol Trolox equivalents per μmol of sample solution.

4. Conclusions

In this study, four new components, (−)-1S-myrothecol (**1a**), (+)-1R-myrothecol (**1b**), methoxy-myrothecol (**2**), and myrothin (**3**), along with four known compounds (**4–7**), were isolated from the deep-sea fungus *Myrothecium* sp. BZO-L062. The enantiomers **1a** and **1b** were purified by chiral HPLC. The absolute configurations of **1a**, **1b**, and **3** were determined by the calculated ECD.

Among these compounds, new compounds **1a** and **1b** showed anti-inflammatory and antioxidant activities at non-toxic concentrations. Derivatives of these compounds could be potent and safe and may be useful for the development of new anti-inflammatory agents.

References

1. Newman, D.J.; Cragg, G.M. Natural products as sources of new drugs over the nearly four decades from 01/1981 to 09/2019. *J. Nat. Prod.* **2020**, *83*, 770–803. [CrossRef]

2. Blunt, J.W.; Carroll, A.R.; Copp, B.R.; Davis, R.A.; Keyzers, R.A.; Prinsep, M.R. Marine natural products. *Nat. Prod. Rep.* **2018**, *35*, 8–53. [CrossRef]

3. Carroll, A.R.; Copp, B.R.; Davis, R.A.; Keyzers, R.A.; Prinsep, M.R. Marine natural products. *Nat. Prod. Rep.* **2020**, *37*, 175–223. [CrossRef] [PubMed]

4. Zhang, P.P.; Deng, Y.L.; Lin, X.J.; Chen, B.; Li, J.; Liu, H.J.; Chen, S.H.; Liu, L. Anti-inflammatory mono- and dimeric sorbicillinoids from the marine-derived fungus *Trichoderma reesei* 4670. *J. Nat. Prod.* **2019**, *82*, 947–957. [CrossRef] [PubMed]

5. El-Kashef, D.H.; Daletos, G.; Plenker, M.; Hartmann, R.; Proksch, P. Polyketides and a dihydroquinolone alkaloid from a marine-derived strain of the fungus *Metarhizium marquandii*. *J. Nat. Prod.* **2019**, *82*, 2460–2469. [CrossRef]

6. Yang, B.Y.; He, Y.; Lin, S.; Zhang, J.W.; Li, H.Q.; Wang, J.P.; Hu, Z.X.; Zhong, Y.H. Antimicrobial dolabellanes and atranones from a marine-derived strain of the toxigenic fungus *Stachybotrys chartarum*. *J. Nat. Prod.* **2019**, *82*, 1923–1929. [CrossRef] [PubMed]

7. Fang, W.; Wang, J.J.; Wang, J.F.; Shi, L.Q.; Li, K.L.; Lin, X.P.; Min, Y.; Yang, B.; Tang, L.; Liu, Y.H.; et al. Cytotoxic and antibacterial eremophilane sesquiterpenes from the marine-derived fungus *Cochliobolus lunatus* SCSIO41401. *J. Nat. Prod.* **2018**, *81*, 1405–1410. [CrossRef]

8. Wen, H.L.; Yang, X.L.; Liu, Q.; Li, S.J.; Li, Q.; Zang, Y.; Chen, C.M.; Wang, J.W.; Zhu, H.C.; Zhang, Y.H. Structurally diverse meroterpenoids from a marine-derived *Aspergillus* sp. fungus. *J. Nat. Prod.* **2019**, *83*, 99–104. [CrossRef]

9. Zhang, Y.H.; Geng, C.; Zhang, X.W.; Zhu, H.J.; Shao, C.L.; Cao, F.; Wang, C.Y. Discovery of bioactive indole-diketopiperazines from the marine-derived fungus *Penicillium brasilianum* aided by genomic information. *Mar. Drugs* **2019**, *17*, 514. [CrossRef]

10. Luo, X.W.; Lin, Y.; Lu, Y.J.; Zhou, X.F.; Liu, Y.H. Peptides and polyketides isolated from the marine sponge-derived fungus *Aspergillus terreus* SCSIO 41008. *Chin. J. Nat. Med.* **2019**, *17*, 149–154. [CrossRef]

11. Chamni, S.; Sirimangkalakitti, N.; Chanvorachote, P.; Saito, N.; Suwanborirux, K. Chemistry of renieramycins. 17. A new generation of renieramycins: Hydroquinone 5-*O*-monoester analogues of renieramycin M as potential cytotoxic agents against non-small-cell lung cancer cells. *J. Nat. Prod.* **2017**, *80*, 1541–1547. [CrossRef] [PubMed]

12. Li, C.J.; Chen, P.N.; Li, H.J.; Mahmud, T.; Wu, D.L.; Xu, J.; Lan, W.J. Potential antidiabetic fumiquinazoline alkaloids from the marine-derived fungus *Scedosporium apiospermum* F41-1. *J. Nat. Prod.* **2020**, *83*, 1082–1091. [CrossRef] [PubMed]

13. Wang, J.J.; Chen, F.M.; Liu, Y.C.; Liu, Y.X.; Li, K.L.; Yang, X.L.; Liu, S.W.; Zhou, X.F.; Wang, J. Spirostaphylotrichin X from a marine-derived fungus as an anti-influenza agent targeting RNA polymerase PB2. *J. Nat. Prod.* **2018**, *81*, 2722–2730. [CrossRef] [PubMed]

14. Wang, L.; Li, M.; Lin, Y.; Du, S.; Liu, Z.; Ju, J.; Suzuki, H.; Sawada, M.; Umezawa, K. Inhibition of cellular inflammatory mediator production and amelioration of learning deficit in flies by deep sea *Aspergillus*-derived cyclopenin. *J. Antibiot.* **2020**, *73*, 622–629. [CrossRef] [PubMed]

15. Zhou, X.; Fang, P.; Tang, J.; Wu, Z.; Li, X.; Li, S.; Wang, Y.; Liu, G.; He, Z.; Gou, D.; et al. A novel cyclic dipeptide from deep marine-derived fungus *Aspergillus* sp. SCSIOW2. *Nat. Prod. Res.* **2016**, *30*, 52–57. [CrossRef] [PubMed]

16. Li, X.F.; Xia, Z.Y.; Tang, J.Q.; Wu, J.H.; Tong, J.; Li, M.J.; Ju, J.H.; Chen, H.R.; Wang, L.Y. Identification and biological evaluation of secondary metabolites from marine derived fungi-*Aspergillus* sp. SCSIOW3, cultivated in the presence of epigenetic modifying agents. *Molecules* **2017**, *22*, 1302. [CrossRef]

17. Wang, L.Y.; Li, M.J.; Tang, J.Q.; Li, X.F. Eremophilane sesquiterpenes from a deep marine-derived fungus, *Aspergillus* sp. SCSIOW2, cultivated in the presence of epigenetic modifying agents. *Molecules* **2016**, *21*, 473. [CrossRef]

18. Macedo, F.C.; Porto, A.L.M.; Marsaioli, A.J. Terreinol—A novel metabolite from *Aspergillus terreus*: Structure and ^{13}C labeling. *Tetrahedron Lett.* **2004**, *45*, 53–55. [CrossRef]

19. Matsui, T.; Kudo, A.; Tokuda, S.; Matsumoto, K.; Hosoyama, H. Identification of a new natural vasorelaxatant compound, (+)-osbeckic acid, from rutin-free tartary buckwheat extract. *J. Agric. Food. Chem.* **2010**, *58*, 10876–10879. [CrossRef]

20. Schmuck, C.; Machon, U. 2-(Guanidiniocarbonyl)furans as a new class of potential anion hosts: Synthesis and first binding studies. *Eur. J. Org. Chem.* **2006**, *19*, 4385–4392. [CrossRef]

21. Steyn, P.S.; Vleggaar, R. The structure of dihydrodeoxy-8-epi-austdiol and the absolute configuration of the azaphilones. *J. Chem. Soc. Perkin Trans. 1* **1976**, 204–206. [CrossRef]

22. Nukina, M.; Marumo, S. Lunatoic acid A and B, aversion factor and its related metabolite of *Cochliobolus lunata*. *Tetrahedron Lett.* **1977**, *18*, 2603–2606. [CrossRef]

23. Bai, Y.; Chang, J.; Xu, Y.; Cheng, D.; Liu, H.; Zhao, Y.; Yu, Z. Antioxidant and myocardial preservation activities of natural phytochemicals from mung bean (*Vigna radiata* L.) seeds. *J. Agric. Food. Chem.* **2016**, *64*, 4648–4655. [CrossRef] [PubMed]

24. Wang, W.; Lee, J.; Kim, K.-J.; Sung, Y.; Park, K.-H.; Oh, E.; Park, C.; Son, Y.-J.; Kang, H. Austalides, osteoclast differentiation inhibitors from a marine-derived strain of the fungus *Penicillium rudallense*. *J. Nat. Prod.* **2019**, *82*, 3083–3088. [CrossRef] [PubMed]

25. Frisch, M.J.; Trucks, G.W.; Schlegel, H.B.; Scuseria, G.E.; Robb, M.A.; Cheeseman, J.R.; Scalmani, G.; Barone, V.; Petersson, G.A.; Nakatsuji, H.; et al. *Gaussian 09 Revision D. 01*; Gaussian Inc.: Wallingford, CT, USA, 2009.

26. Bruhn, T.; Schaumloeffel, A.; Hemberger, Y.; Bringmann, G. SpecDis: Quantifying the comparison of calculated and experimental electronic circular dichroism spectra. *Chirality* **2013**, *25*, 243–249. [CrossRef] [PubMed]

27. Wakamatsu, J.; Stark, T.D.; Hofmann, T. Antioxidative maillard reaction products generated in processed aged garlic extract. *J. Agric. Food. Chem.* **2019**, *67*, 2190–2200. [CrossRef]